LAWRENCE
LIVERMORE
NATIONAL
LABORATORY

UCRL-PROC-215261

Shock Induced (Alpha)-(Epsilon) Phase Change in Iron: Analysis of MD Simulations and Experiment

J. Hawreliak, K. Rosolankova, J. F. Belak, G. Collins, J. Colvin, H. M. Davies, J. H. Eggert, T. C. Germann, B. Holian , D. H. Kalantar, K. Kadau, P. Lomdahl, H. E. Lorenzana, J. Sheppard, J. S. Stolken, J. S. Wark

September 11, 2005

14th APS Conference on Shock Compression of Condensed Matter
Baltimore, MD, United States
July 30, 2005 through August 7, 2005

UCRL-PROC-215261

Shock Induced α-ε phase change in Iron: Analysis of MD simulations and Experiment.

J. Hawreliak[*], K. Rosolankova[†], J.F. Belak[*], G. Collins[*], J. Colvin[*], H.M. Davies[**], J.H. Eggert[*], T.C. Germann[‡], B. Holian[‡], D.H. Kalantar[*], K. Kadau[‡], P. Lomdahl[‡], H.E. Lorenzana[*], J. Sheppard[†], J.S. Stölken[*] and J.S. Wark[†]

[*]*Lawrence Livermore National Laboratory, Livermore, CA 94550*
[†]*University of Oxford, Oxford, UK OX1 3PU*
[**]*AWE, Aldermaston, UK RG7 4PR*
[‡]*Los Alamos National Laboratory, Los Alamos, NM 87545*

Abstract. Multimillion atom non-equilibrium molecular dynamics simulations for shock compressed iron are analyzed using Fourier methods to determine the long scale ordering of the crystal. By analyzing the location of the maxima in k-space we can determine the crystal structure and compression due to the shock. This report presents results from a 19.6GPa simulated shock in single crystal iron and compare them to recent experimental results of shock compressed iron where the crystal structure was determined using in-situ wide angle x-ray diffraction.
Keywords: Phase-Transform,Diffraction,Simulation
PACS: 61.10.NZ,64.70.Kb

INTRODUCTION

Molecular dynamic (MD) simulations are a valuable tool in studying the dynamics of materials under high-strain rate compression [1, 2]. As faster and faster supercomputers become available to today's scientists the amount of material that can be simulated is approaching that which can be studied experimentally. The large amount of data an MD simulations generates presents a new problem "How to interpret the data?", particularly when attempting to connect MD simulations to experiment. Coordination number and radial density functions can be used to calculated the local correlation between atoms. This can be used to simulate diagnostics which are sensitive to local structure, such as extended x-ray absorption fine structure measurements [3]. X-ray diffraction is sensitive to correlation of atoms over longer scale lengths. In this conference proceedings we describe a MD post-processor which takes the Fourier transform of the atomic positions from MD simulations. We will briefly describe how the MD data is post-processed and then looking at one example and compare the post-processed MD result with recent laser shock experiments of iron where the $\alpha - \varepsilon$ phase transition was measured for the first time using wide angle in-situ diffraction.

POST-PROCESSING MD

The MD post-processor (MDPP) performs a Fourier transform on the output of the atomic positions from MD simulations. Previous post-processing of MD data has used a one-dimensional Fourier transform to study specular scattering [4]. Extending this technique to two and three dimensional studies is compu-

tationally expensive, but can provide details which are not obvious in a one-dimensional analysis. The Fourier transform is calculated for a series of delta functions using the sum

$$I(\vec{k}) = \left| \sum_{n=0}^{N-1} e^{i(\vec{k}\cdot\vec{r}_n)} \right|^2, \qquad (1)$$

where $\vec{r}_n$ is the position of the n^{th} atom and N is the total number of atoms in a given test volume or crystal sample. The effect of the finite size of the atoms can be taken into account by use of calculated atomic form factors which are simply a function of distance from the origin in reciprocal space. The periodicity of the crystal structure leads to a periodic intensity pattern in what is known as reciprocal lattice space ($\vec{k}$-space). The solution for a perfect crystal is

$$I(\vec{k}) = \prod_{i=1}^{3} \left(\frac{\sin(N_i \vec{k}\cdot\vec{a}_i)}{\sin(\vec{k}\cdot\vec{a}_i)} \right)^2, \qquad (2)$$

where N_i is the total number of atoms along a particular crystal axis $\vec{a}_i$. However, nothing is ever perfect. It is the interpretation of the deviation from this perfect solution of the reciprocal lattice which leads to understanding what is happening to the MD simulated crystal structure.

Since the transform is calculated numerically the range and dimensionality of $\vec{k}$ is selected to diagnose the desired parameters. This formulation allows one-dimensional study [4] by selecting a particular direction, $\hat{k}$, and by varying the magnitude of $\vec{k}$ along this direction to study a single set of planes. This will give Equ. 2 along a single line in reciprocal space. In the two dimensional case Equ. 2 is calculated on a plane of $\vec{k}$ values [5]. Similarly, the three dimensional case $\vec{k}$ will cover a volume of values, but with each additional dimension the computational cost goes up accordingly.

The MDPP performs the lengthy calculation of a Fourier transform of the atomic positions from the MD simulations because it will give a mapping of the reciprocal lattice space of the the crystal which is recorded experimentally using diffraction. When plotted in units of the reciprocal lattice vectors, the perfect crystal case gives large intensity peaks at the Miller index of the plane from which the diffraction occurs, when the relationship $\vec{k} = \vec{k}_o - \vec{k}_s$ is satisfied, where $\vec{k}_o$ is the wavevector for the incoming beam of x-rays and $\vec{k}_s$ is the wavevector of the diffracted x-rays. For the imperfect crystal it is possible to monitor the change in the crystal structure by the movement of these points which can be compared with experimental data.

APPLICATION TO IRON

Iron is an excellent material to demonstrate the insight into the lattice dynamics the Fourier transform technique offers because of the pressure induced phase transition at 130 kbar [6, 7]. The $\alpha - \varepsilon$ phase transition will generate a change in the long scale-length correlation of the atoms from a BCC crystal strucutre to a HCP crystal structure. This will be obvious in the Fourier transform of the simulation and can also be recorded experimentally using in-situ x-ray diffraction [8]. Figure 1 is a 2-D example of the output of the MDPP using the atomic positions of an 8-million atom NEMD simulation of iron shock compressed to 196 kbar from Kadau *et al.* [9]. The intense peaks give points on the reciprocal lattice, for the uncompressed and compressed BCC as well as the HCP material, because all three materials are present in the simulated sample.

The Fourier transform in Fig. 1 is calculated for the $[001][1\bar{1}0]$ plane (based on the original BCC orientation being shocked along [001]) This plane should show the formation of the hexagonal base structure in the BCC to HCP transformation [10]. In the reciprocal lattice the hexagon is in the same plane as the hexagonal base in real space but rotated about the c-axis by 30^o relative to the orientation of the hexagon in real space [11]. The geometry of the lattice dictates that a uni-axial compression of 18.3% is required for a perfect hexagon to appear in the $[001][1\bar{1}0]$ plane and a shift of alternate planes will create an HCP structure with a c/a ratio of $\sqrt{3}$.

Figure 1 shows that the points corresponding to the BCC lattice off the $[1\bar{1}0]$ axis show three distinct peaks. A sharp peak from the uncompressed material, a second sharp peak at a larger reciprocal lattice vector (corresponding to lattice compression) from the compressed BCC material and a third broader peak from the HCP material. The shift of the BCC points under compression shows movement only in the [001] direction. Showing that in the simulation on this time scale the compression is uni-axial. The

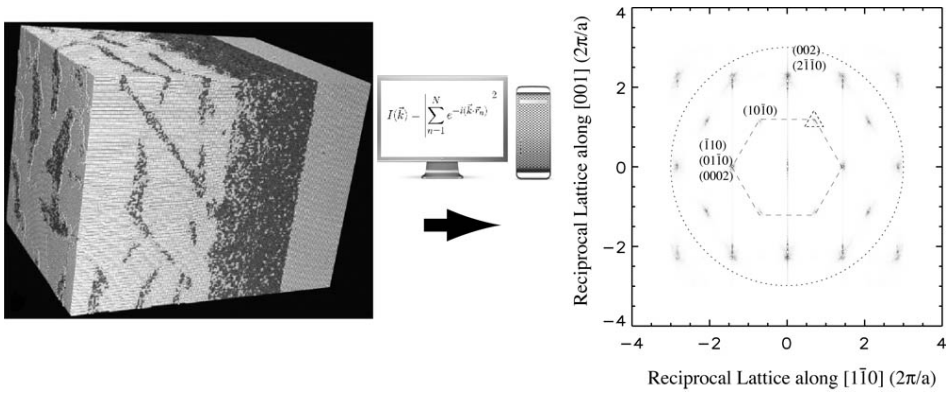

FIGURE 1. This figure schematically shows the method used with the MDPP. The atomic positions from a select portion or entire MD simulation are Fourier transform into reciprocal lattice space. The high intensity peaks represent diffraction planes in the crystal structure. The units are based on the inverse of the original cubic BCC cell. Three points are labeled with the plane labels on the figure. One point contains three labels, to show that there is a BCC component and 2 HCP components, due to the 2 degenerate HCP states. A dashed hexagon shows the reciprocal lattice points are approaching a hexagon. The dotted circle gives the limits that can be probed using K-shell radiation from an iron backlighter.

tell-tale feature of the phase transformation is the appearance of points at $(01\bar{1}0)$, $(11\bar{2}0)$, $(\bar{1}100)$ and similar planes created by the period doubling of the BCC lattice. The hexagonal shape of the new points tells us that the structure is HCP. The dotted circle is the length of the probe vector for K-shell radiation from iron as the Bragg condition limits the region of reciprocal lattice space that can be probed to $|\vec{k}| \leq 2|k_o|$.

Figure 2 is a hi-resolution look at the BCC (002) / HCP $(2\bar{1}\bar{1}0)$ point. The three points correspond to the static material at k_z=2, increasing to k_z=2.14 for 7% compressed material and $k_z = 2.28$ for the phase changed material. Integrating over the $[1\bar{1}0]$ direction makes the peaks more clear, and gives a better idea of the amount of material in each state. The resolution of the two BCC points is determined by the number of atoms in the MD simulation, we can see the affect of a finite number of atoms in the N_i terms in Equ. 2. It is possible but far more computationally expensive to preform a 3D transform and study the complete shape of the points, instead of a single slice. Ideally this could provide information about grain boundaries, dislocations and other crystal defects.

Experimental data in Fig. 2 also shows the two wave structure [8]. The arrows are drawn to the relevant peaks in the experimental data. The two wave structure shows the BCC(002) plane in the uncompressed state, ∼7% compression state, and the same atoms with a ∼14% uniaxial compression but in HCP$(2\bar{1}\bar{1}0)$ plane because of the shift of alternate atomic planes. The other relevant planes are labeled with their BCC orientation (three components) and HCP (four components). Each line in the BCC structure is shown with a BCC label and two HCP labels. This is due to the two degenerate HCP states the crystal can end up in, because whether the planes shift in the [110] direction or the $[1\bar{1}0]$ direction is energetically equivalent, but the plane labels rotate, with some planes begin unique to each orientation. The BCC(002) plane (or any $(00l)$ plane) has the same HCP plane labelled for both HCP orientations because this plane is rotationally symmetric. For BCC(112) there is no diffraction lines from compressed planes associated with the uncompressed diffraction line because of the experimental geometry a shadow was cast in the shocking beam which results in regions of the crystal which are not shocked. This can also be seen in the BCC(002) plane where a region of the curve shows no shock or phase change. There are also two planes unique to a single HCP orientation, HCP$(1\bar{1}00)$ and HCP$(20\bar{2}\bar{1})$, which are due to the period doubling and are unique to the HCP structure. The MD post-processing predicts the HCP$(1\bar{1}00)$ plane, which is in the center of the dashed triangle in Fig. 1.

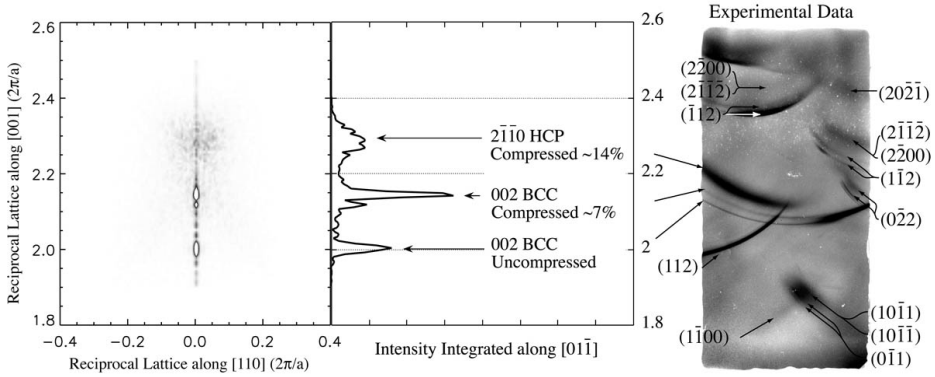

FIGURE 2. A hi-resolution image of the BCC(002) and HCP(2$\bar{1}\bar{1}$0) peaks. It also shows a integration over the [1$\bar{1}$0] direction to give an idea of the widths of the respective peaks. Arrows show the location on experimental film the measurement of each of these peaks. Other diffraction planes are labelled with there plane labels, in both BCC and HCP.

DISCUSSION

With the advent of large MD simulations, which generate large amounts of data there is a need to be able to analyze it in the context of experimental data. A Fourier transform post-processing of the data provides a way to directly compare the MD simulations with experimental x-ray diffraction data. It is particularly useful when using wide angle in-situ x-ray diffraction where many crystal planes can be measured simultaneously effectively mapping out a large region of reciprocal lattice space. This technique has been applied to large non-equilibrium MD simulations in iron and is successful in providing a method to compare the MD simulations with experimental data. It is particularly useful in the case of iron to determine the characteristics in the simulation and experiment that correspond to a phase change. More effort is being put into the development of the techniques to understand the peak broadening mechanisms.

ACKNOWLEDGMENTS

The author would like to thank the staff on Vulcan Laser at the Rutherford Appleton Laboratory where the experimental data presented was taken. This work was conducted under the auspices of the US DOE by the UC LLNL under Contract No. W-7405-Eng-48. Additional support was provided by DOE grants DEFG0398DP00212 and DEFG0300SF2202, by the UK EPSRC Grant GR/R25699/01, and by the LDRD program project 04-ERD-071 at LLNL.

REFERENCES

1. Holian, B. L., and Straub, G. K., *Phys. Rev. Lett.*, **43**, 1598–1600 (1979).
2. Holian, B. L. *et al.*., *Physical Review A (General Physics)*, **22**, 2798–2808 (1980).
3. Rehr, J. J., Albers, R. C., and Zabinsky, S. I., *Phys. Rev. Lett.*, **69**, 3397–3400 (1992).
4. Rosolankova, K. *et al.*., "X-Ray Diffraction from Shocked Crystals: Experiments and Predictions of Molecular Dynamics Simulations," AIP, 2004, vol. 706, pp. 1195–1198.
5. Rosolankova, K., *Picosecond X-ray Diffraction from Shock-Compressed Metals: Experiments and Computational Analysis of Molecular Dynamics Simulations*, Ph.D. thesis, University of Oxford (2005).
6. Bancroft, D., Peterson, E. L., and Minshall, S., *Journal of Applied Physics*, **27**, 291–298 (1956).
7. Jamieson, J., and Lawson, A. W., *Journal of Applied Physics*, **33**, 776–780 (1962).
8. Kalantar, D. H. *et al.*., *Phys. Rev. Lett.*, **95**, 075502 (2005).
9. Kadau, K. *et al.*., *Science*, **296**, 1681–1684 (2002).
10. Wang, F. M., and Ingalls, R., *Physical Review B*, **57**, 5647–5654 (1998).
11. Kittel, C., *Introduction to Solid State Physics*, John Wiley & Sons, Inc, New York, 1976, fifth edn.